

Lewis Acidic Borane Adducts of Pyridines and Stilbazoles for Nonlinear Optics

M. J. Gerald Lesley, Alden Woodward, Nicholas J. Taylor, and Todd B. Marder*

Department of Chemistry, University of Waterloo, Waterloo, Ontario, Canada, N2G 3L1

Irène Cazenobe, Isabelle Ledoux, and Joseph Zyss

Centre National d'Études des Télécommunications-France Telecom, 196, avenue Henri Ravera, BP 107, 92225 Bagneux Cedex, France

Anna Thornton and Duncan W. Bruce

Department of Chemistry, University of Exeter, Exeter, EX4 4QD, U.K.

Ashok K. Kakkar

Department of Chemistry, McGill University, Montreal, Quebec, Canada, H3A 2K6

Received November 17, 1997. Revised Manuscript Received February 10, 1998

A series of neutral pyridyl adducts involving the strong Lewis acids BF_3 and $\text{B}(\text{C}_6\text{F}_5)_3$ has been prepared, and their second-order nonlinear optical coefficients (EFISH method) have been examined. The formation of the pyridyl–boron bond leads to enhancement of the dipole moments and second-order NLO coefficients (β and $\beta(0)$). Reactions of DMAP (4- $\text{Me}_2\text{N}-\text{C}_5\text{H}_4\text{N}$) with BH_3 , BF_3 , and $\text{B}(\text{C}_6\text{F}_5)_3$ give the corresponding neutral pyridine adducts $\text{DMAP}\cdot\text{BH}_3$ (orthorhombic, $Pbca$, $a = 9.6914(7)$ Å; $b = 11.7173(9)$ Å; $c = 22.718(2)$ Å; $V = 1622.4(5)$ Å³; $Z = 8$; $\rho = 1.114$ g cm⁻³), $\text{DMAP}\cdot\text{BF}_3$ (orthorhombic, $Pbca$, $a = 10.430(3)$ Å; $b = 8.111(2)$ Å; $c = 20.295(7)$ Å; $V = 1717.0(9)$ Å³; $Z = 8$; $\rho = 1.470$ g cm⁻³), and $\text{DMAP}\cdot\text{B}(\text{C}_6\text{F}_5)_3$ (orthorhombic, $Pbca$, $a = 12.322(1)$ Å; $b = 20.556(2)$ Å; $c = 28.455(3)$ Å; $V = 7207.4(14)$ Å³; $Z = 8$; $\rho = 1.508$ g cm⁻³). Reactions of $\text{Me}_2\text{N}-4-\text{C}_6\text{H}_4-\text{CH}=\text{CH}-\text{C}_5\text{H}_4\text{N}$, $\text{MeO}-4-\text{C}_6\text{H}_4-\text{CH}=\text{CH}-\text{C}_5\text{H}_4\text{N}$, and $\text{Me}_2\text{N}-4-\text{C}_6\text{H}_4-\text{C}\equiv\text{C}-\text{C}_5\text{H}_4\text{N}$ with BF_3 and $\text{B}(\text{C}_6\text{F}_5)_3$ result in materials that are highly luminescent and incorporate structural features that are known to give rise to large second-order NLO effects. X-ray diffraction analysis for the compound $\text{Me}_2\text{N}-4-\text{C}_6\text{H}_4-\text{C}\equiv\text{C}-\text{C}_5\text{H}_4\text{N}\cdot\text{B}(\text{C}_6\text{F}_5)_3$ (monoclinic, $P2_1/c$, $a = 9.883(2)$ Å; $b = 10.717(1)$ Å; $c = 28.421(4)$ Å; $\beta = 91.96(1)^\circ$; $V = 2993.4(8)$ Å³; $Z = 4$; $\rho = 1.629$ g cm⁻³) is also described.

Introduction

New organic materials with extended π -conjugation have been studied extensively in attempts to prepare materials with high thermal stability and efficient nonlinear optical (NLO) responses which are superior to inorganic crystalline materials.^{1,2} Recently, Marder et al.³ have reviewed the use of stilbazolium salts which have been shown to exhibit some of the largest second-order NLO responses while remaining stable to tem-

peratures well over 250 °C, as required for device manufacture. The stilbazolium compounds, however, are not well suited to poling⁴ into polymer hosts due to their ionic nature. We decided to examine the effect of binding Lewis-acidic boranes to stilbazoles and related

* To whom correspondence should be addressed at Department of Chemistry, South Road, University of Durham, Durham, England DH1 3LE. Phone: 44-191-374-3137. Fax: 44-191-386-1127. E-mail: Todd.Marder@durham.ac.uk.

(1) For reviews on materials for NLO see: (a) *Nonlinear Optical Properties of Organic and Polymeric Materials*; Williams, D. J., Ed.; ACS Symp. Ser. 233; American Chemical Society: Washington, DC, 1983. (b) *Nonlinear Optical Properties of Organic Molecules and Crystals*; Vol. 1, 2. Chemla, D. S., Zyss, J., Eds.; Academic Press: New York, 1987. (c) *Organic Materials for Nonlinear Optics*; Hahn, R. A., Eds.; Spec. Publ. No. 69; The Royal Society of Chemistry: London, 1989. (d) *Organic Materials for Nonlinear Optics II*; Hahn, R. A., Bloor, D., Eds.; Spec. Publ. No. 91; The Royal Society of Chemistry: Cambridge, 1991. (e) Prasad, P. N.; Williams, D. J. *Introduction to Nonlinear Optical Effects in Molecules and Polymers*; Wiley: Chichester, 1991. (f) Nalwa, H. S.; Miyata, S. *Nonlinear Optics of Organic Molecules and Polymers*; CRC Press: Boca Raton, FL, 1994.

(2) For reviews involving applications of NLO materials see: (a) *Conjugated Polymeric Materials: Opportunities in Electronics, Optoelectronics, and Molecular Electronics*; Bredas, J. L., Chance, R. R., Eds.; NATO ARW Series E182; Kluwer Academic Publishers: Dordrecht, 1990. (b) *Materials for Nonlinear Optics: Chemical Perspectives*; Marder, S. R., Sohn, J. E., Stucky, G. D., Eds.; ACS Symp. Ser. 455; American Chemical Society: Washington, DC, 1991. (c) *Molecular Nonlinear Optics: Materials, Physics, and Devices*; Zyss, J., Ed.; Academic Press: New York, 1994. (d) *Nonlinear Optical Properties of Organic Materials VII*; Mohlmann, G. R., Ed.; Proc. SPIE, Vol. 2285; The International Society for Optical Engineering: Washington, DC, 1994. (e) *Organic, Metallo-Organic, and Polymeric Materials for Nonlinear Optical Applications*; Marder, S. R., Perry, J. W., Eds.; Proc. SPIE, Vol. 2143; The International Society for Optical Engineering: Washington, DC, 1994.

(3) Marder, S. R.; Perry, J. W.; Yakymyshyn, C. P. *Chem. Mater.* **1994**, *6*, 1137.

(4) For discussions of poling experiments with polymers see, for example: (a) Hubbard, M. A.; Marks, T. J.; Yang, J. Y.; Wong, G. K. *Chem. Mater.* **1989**, *1*, 167. (b) Xu, C.; Wu, B.; Dalton, L. R.; Shi, Y.; Ranon, P. M.; Steier, W. H. *Macromolecules* **1992**, *25*, 6714. (c) *Ibid.* **1992**, *25*, 6716. (d) Gilmour, S.; Montgomery, R. A.; Marder, S. R.; Cheng, L.-T.; Jen, A. K.-Y.; Cai, Y.; Perry, J. W.; Dalton, L. R. *Chem. Mater.* **1994**, *6*, 1603.

aryl and alkynyl derivatives in an attempt to create a strong donor/acceptor arrangement while maintaining the neutrality of the compounds.

The change in dipole moment upon excitation is an important consideration since the magnitude of the overall nonlinear response is proportional to this quantity. Thus, a large change in the dipole moment of the molecule between the ground and excited states is desirable. This is often achieved synthetically by the incorporation of a strong π -donor/acceptor arrangement at the ends of the molecule which leads to a charge-transfer excited state. The extended π -electron system linking these substituents has also been studied. A large number of compounds that have been designed previously include a combination of aryl, olefinic, and alkynyl moieties to facilitate intramolecular charge-transfer (ICT) transitions. For example, we have recently reported studies involving the synthesis and nonlinear optical characterization of a series of BPEB (bis(phenylethynyl)benzene) derivatives, as well as related Pt(PMe₂Ph)₂ analogues^{5b} to compare the efficiency of the metal center with that of the benzene moiety, for communication between the ends of the molecules.^{5c,d} The use of stilbene, stilbazole, and related azobenzene derivatives^{3,4,6} generally gives rise to larger NLO responses compared to the alkynyl derivatives;^{5,7} however, the former exhibit red-shifted absorptions in the region of the frequency-doubled radiation which is not desirable for second harmonic generation. The use of the stilbazole moiety as a π -system has dominated much of the current research in this area since the incorporation of the heteroatom (N) reduces the aromatic stabilization in these compounds making the charge-transfer excited state more accessible. In addition, it has been found that extending the π -conjugation of the systems gives rise to larger NLO responses due to the lowering of the energy of the excited states and to the increase of the oscillator strength (hyperchromic effect).⁹

Although large single crystals are desirable to quantify the various tensor components of the responses³

and for certain applications, the future of NLO will certainly lie in the ability to incorporate these chromophores into polymers that can be easily poled and fabricated as thin films (ca. 1 μ m). Several groups have examined the poling of chromophores into polymers by applying a dc-electric field upon heating the polymer above the glass transition temperature. The material is then cooled to room temperature with the electric field applied, thereby locking the chromophores into a statistical dipolar arrangement of molecular dipoles.^{4b,c} Covalent attachment of the chromophore to polymer side chains has also been examined to ensure a better orientational stability of oriented dipoles at room or moderate (<85 °C) temperatures.^{4a,d} The utility of this technique often depends on the thermal stability of the chromophores. Typically, the chromophore must be stable at temperatures greater than 200 °C for periods of several hours.^{4d}

The incorporation of a strong donor/acceptor arrangement has been achieved by the quaternization of the pyridyl functionality using a variety of reagents. The stilbazolium salts obtained were highly efficient materials in terms of their second-order NLO responses in the solid state, and the magnitude of the response was reported to be highly dependent on the counterion which was incorporated into the structure. For example, the compound DAST ((*N,N*-dimethylamino)-*N*-methylstilbazolium *p*-toluenesulfonate) was reported to have a powder SHG efficiency 1000 times that of the standard, urea. This value was substantially larger than those for previously characterized stilbazolium salts ($X^- = \text{CH}_3\text{SO}_3^-$ ($\chi^{(2)} = 220 \times \text{urea}$); BF_4^- ($\chi^{(2)} = 75 \times \text{urea}$)).¹⁰ The value $\chi^{(2)}$ represents the second-order susceptibility coefficient. This value is derived from experiments in which the bulk solid is analyzed and is applicable only to compounds that crystallize in acentric space groups. The stilbazolium salts incorporating Cl^- and CF_3SO_3^- counterions crystallize in centric space groups and thus have $\chi^{(2)}$ values of 0. The drastic effect of the counterion on values of $\chi^{(2)}$ has been attributed to the ability of the counterion to screen chromophores from one another and the inherent Coulombic forces between ions, which minimizes bipolar interactions thought to favor formation of crystals in centric space groups.

It is of interest that related studies involving julolidine–stilbazolium salts were found to result in moderate $\chi^{(2)}$ values.¹¹ The julolidyl functionality was expected to result in more efficient π -donation by allowing more efficient overlap with the aromatic ring and by virtue of the ortho-substitution, which had been shown to result in increased values of $\chi^{(2)}$ in related derivatives (*p*-nitroaniline; $\beta = 35 \times 10^{-30}$ esu vs MNA (2-methyl-4-nitroaniline); $\beta = 42 \times 10^{-30}$ esu). In this case, incorporation of the julolidyl functionality had a pronounced effect resulting in $\chi^{(2)}$ values that were less than that of the standard, urea. Unfortunately, experi-

(5) (a) Nguyen, P.; Yuan, Z.; Agocs, L.; Lesley, G.; Marder, T. B. *Inorg. Chim. Acta* **1994**, *220*, 289. (b) Marder, T. B.; Lesley, G.; Yuan, Z.; Fyfe, H. B.; Chow, P.; Stringer, G.; Jobe, I. R.; Taylor, N. J.; Williams, I. D.; Kurtz, S. K. In ref 2b, p 605. (c) Nguyen, P.; Lesley, G.; Dai, C.; Taylor, N. J.; Marder, T. B.; Chu, V.; Viney, C.; Ledoux, I.; Zyss, J. In *Applications of Organometallic Chemistry in the Preparation and Processing of Advanced Materials*; Harrod, J. F., Laine, R. M., Eds.; NATO ASI Series E; Kluwer Academic Publishers: Dordrecht, 1995; Vol. 297, p 333. (d) Nguyen, P.; Lesley, G.; Marder, T. B.; Ledoux, I.; Zyss, J. *Chem. Mater.* **1997**, *9*, 406.

(6) (a) Cheng, L.-T.; Tam, W.; Marder, S. R.; Steigman, A. E.; Rikken, G. *J. Phys. Chem.* **1991**, *95*, 10631. (b) *Ibid.* **1991**, *95*, 10634. (c) Dirk, C. W.; Katz, H. E.; Schilling, M. L.; King, L. A. *Chem. Mater.* **1990**, *2*, 700. (d) Jen, A. K.-Y.; Rao, V. P.; Wong, K. Y.; Drost, K. J. *J. Chem. Soc., Chem. Commun.* **1993**, 90. (e) Rao, V. P.; Jen, A. K.-Y.; Wong, K. Y.; Drost, K. J. *Ibid.* **1993**, 1118. (f) Rao, V. P.; Cai, Y. M.; Jen, A. K.-Y. *Ibid.* **1994**, 1689. (g) Jen, A. K.-Y.; Rao, V. P.; Drost, K. J.; Wong, K. Y.; Cava, M. P. *Ibid.* **1994**, 2057.

(7) (a) Kurihara, T.; Tabei, H.; Kaino, T. *J. Chem. Soc., Chem. Commun.* **1987**, 959. (b) Tabei, H.; Kurihara, T.; Kaino, T. *Appl. Phys. Lett.* **1987**, *50*, 185. (c) Steigman, A. E.; Miskowski, W. M.; Perry, K. J.; Coulter, D. R. *J. Am. Chem. Soc.* **1987**, *109*, 5884. (d) Steigman, A. E.; Graham, E. M.; Perry, K. J.; Khundkar, L. R.; Cheng, L.-T.; Perry, J. W. *J. Am. Chem. Soc.* **1991**, *113*, 7658. (e) Perry, J. W.; Steigman, A. E.; Marder, S. R.; Coulter, D. R.; Beratan, D. N.; Brinza, D. E.; Klavetter, F. L.; Grubbs, R. H. In *Nonlinear Optical Properties of Organic Materials*; Proc. SPIE, Vol. 971; The International Society for Optical Engineering: Washington, DC, 1988; p 17. (f) Steigman, A. E.; Perry, J. W.; Cheng, L.-T. In ref 1d, p 149. (g) Dehu, C.; Meyers, F.; Brédas, J. L. *J. Am. Chem. Soc.* **1993**, *115*, 6198.

(8) (a) Etter, M. C.; Frankenbach, G. M. *Chem. Mater.* **1989**, *1*, 10. (b) Etter, M. C.; Huang, K. S.; Frankenbach, G. M.; Admond, D. A. In ref 2b, p 457. (c) Etter, M. C. *J. Phys. Chem.* **1991**, *95*, 4601.

(9) (a) Blanchard-Desce, M.; Ledoux, I.; Lehn, J.-M.; Maithe, J.; Zyss, J. *J. Chem. Soc., Chem. Commun.* **1988**, 737. (b) Blanchard-Desce, M.; Lehn, J.-M.; Ledoux, I.; Zyss, J. In ref 1c, p 170. (c) Zyss, J.; Ledoux, I.; Nicoud, J.-F. In ref 2c, p 129. (d) Marder, S. R.; Cheng, L.-T.; Tiemann, B. G.; Friedli, A. C.; Blanchard-Desce, M.; Perry, J. W.; Skindhoj, J. *Science* **1994**, *263*, 511.

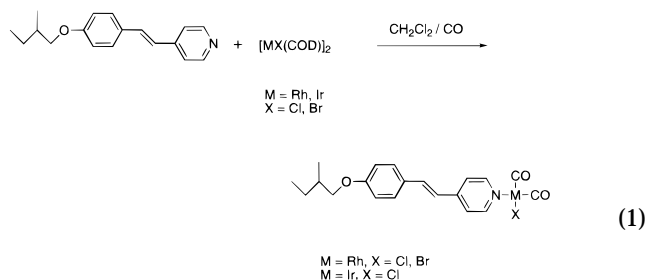
(10) Meredith, G. R. In ref 1a, p 27.

(11) Bruce, D. W.; Denning, R. G.; Grayson, M. G.; Le Lagadec, R.; Lai, K. K.; Pickup, B. T.; Thornton, A. *Adv. Mater. Opt. Electron.* **1994**, *4*, 293.

mental techniques involving the determination of β were not suited to these and related salts since EFISH methods present inherent problems associated with conduction of the salts when an external dc field is applied and hyper-Raleigh scattering techniques were unavailable. Clearly, the formation of neutral analogues would not be hindered by such restrictions.

The coordination of electron-withdrawing metal complexes to pyridine and bipyridine derivatives has been studied by several researchers.¹² Tam et al. (Figure 1) prepared a series of neutral, metal pyridyl derivatives by the coordination of the $W(CO)_5$ moiety.^{12a,b} This was shown to increase both the dipole moment of the molecules as well as the values of β . These compounds were examined because the complexes were known to have their charge-transfer axis along the dipole direction making them ideal for the EFISH study of the β values upon modification of the ligand and metal center. The coordination of the metal fragment was shown to increase the value of β by as much as 50 times that of the parent chromophore. For example, the 4-acetylpyridine derivative exhibited a β value of -9.3×10^{-30} esu while the parent molecule displayed values of $<0.2 \times 10^{-30}$ esu. The negative sign for β has been explained as the result of a reduction of the dipole moment upon excitation.^{12c}

Neutral, transition-metal derivatives of stilbazole compounds have also been studied and were shown to result in enhanced values of the second-order NLO responses when compared to the parent chromophores.^{12a,d,13a} The π -acceptor substituted $W(CO)(4\text{-X-styrylpyridine})$ ($X = H, COH, NO_2$) compounds resulted in only modest values of $\mu\beta$ ^{12a} while the π -donor substituted derivative ($X = NMe_2$) was shown to result in an increase in $\mu\beta$ of 5 times the uncomplexed chromophore.^{12d} The alkoxy derivative (eq 1) ($\mu\beta = 60$



$\times 10^{-48}$ esu) was found^{13b} to exhibit larger values for μ and β upon coordination of all the metal fragments examined. The largest increase was present for the $Ir(CO)_2Br$ complex, which possessed a $\mu\beta$ value (184×10^{-48} esu) approximately 3 times that of the parent chromophore. Similar derivatives involving additional metal complexes have been examined as liquid-crystalline materials.^{13c}

(12) (a) Cheng, L.-T.; Tam, W.; Eaton, D. F. *Organometallics* **1990**, *9*, 2856. (b) Cheng, L.-T.; Tam, W.; Meredith, G. R. *Mol. Cryst. Liq. Cryst.* **1990**, *189*, 137. (c) The NLO properties of these and related compounds have recently been described in ref 13c, p 144. (d) Kanis, D. R.; Lacroix, P. G.; Ratner, M. A.; Marks, T. J. *J. Am. Chem. Soc.* **1994**, *116*, 10089.

(13) (a) Bruce, D. W.; Thornton, A. *Mol. Cryst. Liq. Cryst.* **1993**, *231*, 253. (b) Bruce, D. W.; Dunmur, D. A.; Lalinde, E.; Maitlis, P. M.; Styring, P. *Liq. Cryst.* **1988**, *3*, 385. (c) The liquid-crystalline properties of related materials have been recently reviewed: *Inorganic Materials*, 2nd Ed.; Bruce, D. W., O'Hare D., Ed.; John Wiley and Sons: Chichester, England, 1996; Chapter 8.

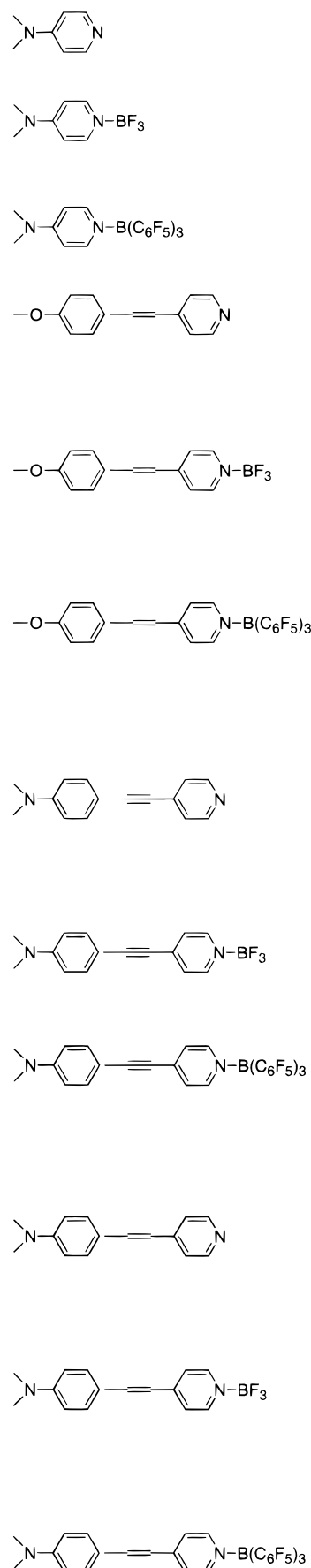
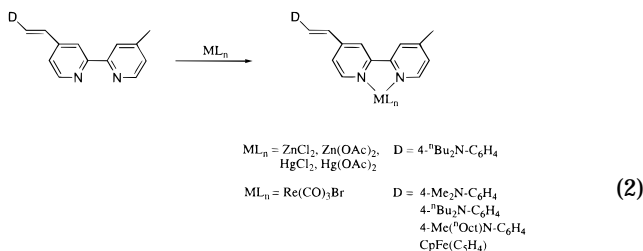


Figure 1. Metal pyridyl compounds for second-order NLO.

Le Bozec et al. have examined similar effects in the synthesis of metal-4,4'-unsymmetrically substituted,

2,2'-bipyridyl derivatives (eq 2).^{14a} Similar studies of



coordination to polymeric materials involving bipyridyl groups have also been reported.^{14b} EFISH measurements were carried out for a series of different metal derivatives.^{14a} The variation of the ligand-donor substituent in the various $Re(CO)_3Br$ derivatives was not studied in this regard. The molecular hyperpolarizability (β) was found to increase by as much as a factor of 9 for the $ZnCl_2$ derivative ($\beta = 152.0 \times 10^{-30}$ esu) when compared to the value obtained for the uncomplexed chromophore ($\beta = 13.7 \times 10^{-30}$ esu).

We and others have also recently studied the second-order NLO properties of several series of functionalized organoboranes.¹⁵ These studies examined the effect of push-pull organoboranes for second- and third-order NLO effects, as well as symmetric bis(dimesitylboryl) compounds for third-order NLO effects. The increase in the NLO efficiencies of chromophores attached to Lewis-acidic metal complexes noted above is an indication that the related Lewis-acidic borane adducts should be capable of such effects. We now report the synthesis and characterization of a series of neutral, highly polar, borane adducts of DMAP, two stilbazole derivatives, and the related alkynyl analogue.

Experimental Section

General Techniques. All reactions were performed at room temperature in a nitrogen-filled glovebox. Common solvents were dried using the appropriate drying agents and distilled under an N_2 atmosphere: toluene, diethyl ether, THF from Na/benzophenone, hexanes from Na metal, and $CHCl_3$ from CaH_2 . The NMR solvents $CDCl_3$ and CD_2Cl_2 were distilled from CaH_2 following three freeze/pump/thaw cycles. Melting point determinations were made using a Mel-Temp II (Laboratory Devices) apparatus equipped with a Fluke 51 thermocouple (John Fluke Mfg. Co., Inc.) with samples sealed in glass capillary tubes using wax.

The following chemicals were obtained commercially and used without further purification: (Aldrich Chemicals) 4-(*N,N*-dimethylamino)pyridine (DMAP), borane (BH_3 , 1 M in THF), and trifluoroborane etherate ($BF_3 \cdot Et_2O$, 1 M in diethyl ether). The compounds tris(perfluorophenyl)borane ($B(C_6F_5)_3$), 4-methoxy-4'-stilbazole, and 4-(*N,N*-dimethylamino)-4'-stilbazole were prepared by known synthetic routes.¹⁶

(14) (a) Bourgault, M.; Mountassir, C.; Le Bozec, H.; Ledoux, I.; Pucetti, G.; Zyss, J. *J. Chem. Soc., Chem. Commun.* **1993**, 1623. (b) Peng, Z.; Yu, L. *J. Am. Chem. Soc.* **1996**, *118*, 3777.

(15) (a) Yuan, Z.; Taylor, N. J.; Marder, T. B.; Williams, I. D.; Kurtz, S. K.; Cheng, L.-T. *J. Chem. Soc., Chem. Commun.* **1990**, 1489. (b) Yuan, Z.; Taylor, N. J.; Marder, T. B.; Williams, I. D.; Kurtz, S. K.; Cheng, L.-T. In ref 1d, p 190. (c) Yuan, Z.; Taylor, N. J.; Sun, Y.; Marder, T. B.; Williams, I. D.; Cheng, L.-T., *J. Organomet. Chem.* **1993**, *449*, 27. (d) Yuan, Z.; Taylor, N. J.; Marder, T. B.; Cheng, L.-T., manuscript in preparation. (e) Yuan, Z.; Taylor, N. J.; Ramachandran, R.; Marder, T. B. *Appl. Organomet. Chem.* **1996**, *10*, 305. (f) Lequan, M.; Lequan, R. M.; Ching, K. C. *J. Mater. Chem.* **1991**, *1*, 997. (g) Lequan, M.; Lequan, R. M.; Ching, K. C.; Barzoukas, M.; Fort, A.; Lahoucine, H.; Bravie, G.; Chasseau, D.; Gaultier, J. *J. Mater. Chem.* **1992**, *2*, 719.

Nuclear magnetic resonance experiments were performed on Bruker AC200 or AMX 500 spectrometers at the following frequencies: 1H 200 and 500 MHz; $^{13}C\{^1H\}$ 50 and 125 MHz; $^{11}B\{^1H\}$ 64 MHz; $^{19}F\{^1H\}$ 188 MHz, unless otherwise stated. The 1H chemical shifts were referenced to the internal standard tetramethylsilane (TMS) and ^{13}C chemical shifts were referenced to the solvent resonances as an internal standard. The ^{11}B and ^{19}F chemical shifts were referenced to the external standards $F_3B \cdot OEt_2$ and trifluoroacetic acid (TFA in $CDCl_3 = -76.53$ ppm), respectively. The ^{11}B NMR spectra were obtained using a background subtraction routine to remove resonances due to borosilicate glass in the NMR probe and NMR tube. This was accomplished by recording the spectrum of an NMR tube containing the same height of pure solvent and with collection parameters identical to that of the sample and subtracting this background FID from that of the sample. All spectra were recorded in $CDCl_3$ and coupling constants are given in hertz unless otherwise stated. UV/vis spectra ($CHCl_3$) were measured on a Hewlett-Packard 8452A diode array spectrophotometer using standard, dual-window, quartz cells ($l = 10$ mm). Elemental analyses were obtained from M-H-W Laboratories, Phoenix, AZ, or Bristol University, Bristol, UK.

EFISH measurements were carried out at 1.34 μm using a Q-switched, mode-locked Nd^{3+} :YAG laser emitting pulse trains of 160 ps duration within a whole temporal envelope of 90 ns. Dipole moment measurements were carried out using the standard Guggenheim method.¹⁷

Characterization of Compounds

$B(C_6F_5)_3$ (1b). $^{13}C\{^1H\}$ NMR (50 MHz) δ 148.3 (d, $J_{CF} = 245$ Hz), 145.2 (d, $J_{CF} = 247$ Hz), 138.2 (d, $J_{CF} = 242$ Hz), 112.9 (s, broad); $^{11}B\{^1H\}$ (64 MHz) δ 0.3 (s); $^{19}F\{^1H\}$ (188 MHz) δ -128.5 (m, 2F), -143.3 (t, 1F, $J_{FF} = 19.6$ Hz), -160.6 (m, 2F).

4-Me₂N-C₅H₄N (DMAP, 2). 1H NMR (200 MHz) δ 8.14 (d, AA'XX', H₂ and H₆, $^3J_{HH} = 6.5$ Hz), 6.39 (d, AA'XX', H₃ and H₅, $^3J_{HH} = 6.5$ Hz), 2.89 (s, H₇); $^{13}C\{^1H\}$ NMR (50 MHz), δ 154.1 (C₄), 149.7 (C₂ and C₆), 106.5 (C₃ and C₅), 38.9 (C₇).

trans-4-MeO-C₆H₄-C(H)=C(H)-C₅H₄N (3). Mp 135.1–136.2 °C. 1H NMR (200 MHz) δ 8.53 (d, AA'XX', H₂ and H₆, $^3J_{HH} = 6.1$ Hz), 7.45 (d, AA'XX' H₁₁ and H₁₃, $^3J_{HH} = 8.8$ Hz), 7.30 (d, AA'XX', H₃ and H₅, $^3J_{HH} = 6.1$ Hz), 7.23 (d, AB, H₇, $^3J_{HH} = 16.2$ Hz), 6.89 (d, AA'XX', H₁₀ and H₁₄, $^3J_{HH} = 8.8$ Hz), 6.84 (d, AB, H₈, $^3J_{HH} = 16.2$ Hz), 3.81 (s, H₁₅); $^{13}C\{^1H\}$ NMR (50 MHz), δ 160.1 (C₁₂), 150.1 (C₂ and C₆), 144.9 (C₄), 132.6 (C₈), 128.9 (C₉), 128.3 (C₁₀ and C₁₄), 123.7 (C₇), 120.6 (C₃ and C₅), 114.2 (C₁₁ and C₁₃), 55.3 (C₁₅).

trans-4-Me₂N-C₆H₄-C(H)=C(H)-C₅H₄N (4). Mp 244.5–244.9 °C (d). 1H NMR (200 MHz) δ 8.48 (d, AA'XX', H₂ and H₆, $^3J_{HH} = 6.1$ Hz), 7.41 (d, AA'XX', H₁₁ and H₁₃, $^3J_{HH} = 8.8$ Hz), 7.28 (d, AA'XX', H₃ and H₅, $^3J_{HH} = 6.1$ Hz), 7.22 (d, H₇, AB, $^3J_{HH} = 16.5$ Hz), 6.77 (d, AB, H₈, $^3J_{HH} = 16.5$ Hz), 6.69 (d, AA'XX', H₁₀ and H₁₄, $^3J_{HH} = 8.8$ Hz), 2.99 (s, H₁₅); $^{13}C\{^1H\}$ NMR (50 MHz), δ 150.8 (C₁₂), 150.0 (C₂ and C₆), 145.5 (C₄), 133.3 (C₈), 128.3 (C₁₀ and C₁₄), 124.2 (C₉), 121.2 (C₇), 120.3 (C₃ and C₅), 112.1 (C₁₁ and C₁₃), 40.3 (C₁₅).

Synthesis of Compounds

4-Me₂N-C₆H₄-C≡C-C₅H₄N (5). A 250 mL round-bottom flask was charged with 4-C₅H₄N-C≡CH (337 mg, 3.27 mmol), 4-(CH₃)₂N-C₆H₄I (807 mg, 3.27 mmol), and a catalytic amount of $PdCl_2(PPh_3)_2$ (23 mg, 1 mol %, 3.27×10^{-2} mmol) and CuI (12.5 mg, 2 mol %, 6.54×10^{-2} mmol). Freshly distilled 3Pr_2NH (20 mL) was added, and the reaction mixture stirred at ambient temperature for 3 h. The resulting mixture was reduced in vacuo and purified by column chromatography (neutral, Beckmann 1, 150 mesh) using diethyl ether as eluant. The light yellow elution band was reduced in vacuo and

(16) For the preparation of $B(C_6F_5)_3$ see: Massey, A. G.; Park, A. J. *J. Organomet. Chem.* **1964**, *2*, 245. For the stilbazole reagents see refs 3 and 13b.

(17) Guggenheim, E. A. *Trans. Faraday Soc.* **1949**, *45*, 203.

recrystallized from diethyl ether/hexanes to give a yellow solid (5, 438 mg, 60%). Mp 185.0–187.0 °C (d). Anal. Calcd for $C_{15}H_{14}N_2$: C, 81.05; H, 6.35; N, 12.60. Found: C, 79.94; H, 7.13; N, 12.15. 1H NMR (200 MHz) δ 8.55 (d, AA'XX', H₂ and H₆, $^3J_{HH}$ = 6.1 Hz), 7.43 (d, AA'XX', H₁₁ and H₁₃, $^3J_{HH}$ = 9.0 Hz), 7.33 (d, AA'XX', H₃ and H₅, $^3J_{HH}$ = 6.0 Hz), 6.66 (d, AA'XX', H₁₀ and H₁₄, $^3J_{HH}$ = 9.0 Hz), 3.01 (s, H₁₅); $^{13}C\{^1H\}$ NMR (50 MHz), δ 149.9 (C₂ and C₆), 133.2 (C₁₀ and C₁₄), 125.2 (C₃ and C₅), 118.8 (C₁₁ and C₁₃), 40.1 (C₁₅).

DMAP·BF₃ (6a). A solution of BF₃·Et₂O (**1a**, 1.0 M, 5.0 mL, 5.0 mmol) was added dropwise via pipet to a stirred solution of DMAP (**2**, 500 mg, 4.09 mmol) in THF (5 mL). The reaction mixture was stirred for 3 h at ambient temperature, and the precipitate was isolated by vacuum filtration (648 mg, 83%). Mp 129.8–130.9 °C. Anal. Calcd for C₇H₁₀BF₃N₂: C, 44.26; H, 5.31; N, 14.75. Found: C, 44.18; H, 5.46; N, 14.71. 1H NMR (200 MHz) δ 8.09 (d, broad, AA'XX', H₂ and H₆), 6.61 (d, AA'XX', H₃ and H₅, $^3J_{HH}$ = 7.0 Hz), 3.16 (s, H₇); $^{13}C\{^1H\}$ NMR (50 MHz) δ 156.6 (C₄), 141.8 (C₂ and C₆), 106.4 (C₃ and C₅), 39.6 (C₇); $^{11}B\{^1H\}$ (64 MHz) δ 0.34 (s, broad); $^{19}F\{^1H\}$ (188 MHz) δ -152.7 (m).

DMAP·B(C₆F₅)₃ (6b). A solution of B(C₆F₅)₃ (**1b**, 126 mg, 0.246 mmol) in toluene (5 mL) was added dropwise via pipet to a stirred solution of DMAP (**2**, 30 mg, 0.246 mmol) in toluene (5 mL). The reaction mixture was stirred overnight at ambient temperature and was reduced in vacuo to ca. 2 mL. The addition of hexanes (10 mL) to the viscous mixture resulted in the formation of a white precipitate that was isolated by vacuum filtration (156 mg, 85%). Mp 225.2–226.5 °C (d). Anal. Calcd for C₂₅H₁₀BF₁₅N₂: C, 47.51; H, 1.59; N, 4.42. Found: C, 47.24; H, 1.40; N, 3.78. 1H NMR (200 MHz) δ 7.93 (d, broad, AA'XX', H₂ and H₆), 6.55 (d, AA'XX', H₃ and H₅, $^3J_{HH}$ = 7.0 Hz), 3.17 (s, H₇); $^{13}C\{^1H\}$ NMR (50 MHz) δ 155.5 (C₄), 147.7 (dm, J_{C-F} = 260 Hz, BR₃), 145.1 (C₂ and C₆), 139.7 (dm, J_{C-F} = 270 Hz, BR₃), 136.8 (dm, J_{C-F} = 270 Hz, BR₃), 106.1 (C₃ and C₅), 39.5 (C₇); (minute resonances attributed to toluene were also apparent; B–C resonances were not observed); $^{11}B\{^1H\}$ (64 MHz) δ -5.3 (s); $^{19}F\{^1H\}$ (188 MHz) δ -131.7 (m, 2F), -157.6 (t, broad, 1F), -163.5 (m, 2F).

DMAP·BH₃ (6c). A solution of BH₃ (**1c**, 0.80 mL, 1 M in THF, 0.8 mmol) was added dropwise via pipet to a stirred solution of DMAP (**2**, 96 mg, 0.80 mmol) in toluene (5 mL). The reaction mixture was stirred overnight at ambient temperature and the white precipitate was isolated by filtration. Mp 166.2–167.8 °C. 1H NMR (CDCl₃, 200 MHz) δ 7.93 (d, AA'XX', H₂ and H₆, $^3J_{HH}$ = 7.2 Hz), 6.46 (d, AA'XX', H₃ and H₅, $^3J_{HH}$ = 7.2 Hz), 3.06 (s, H₇), ca 1.3 (s, broad, BH₃); $^{13}C\{^1H\}$ NMR (CD₂Cl₂, 50 MHz) δ 154.9 (C₄), 146.7 (C₂ and C₆), 106.5 (C₃ and C₅), 39.6 (C₇); $^{11}B\{^1H\}$ (CDCl₃, 64 MHz) δ -13.8 (s).

trans-4-MeO-C₆H₄-C(H)=C(H)-C₅H₄N·BF₃ (7a). A solution of BF₃·Et₂O (**1a**, 0.8 M, 1.8 mL, 1.4 mmol) was added dropwise via pipet to a stirred solution of *trans*-4-MeO-C₆H₄-C(H)=C(H)-C₅H₄N (**3**, 300 mg, 1.42 mmol) in THF (5 mL). The reaction mixture was stirred overnight at ambient temperature while covered in aluminum foil. The reaction mixture was vacuum filtered to remove a small amount of precipitate that had formed. The filtrate portion was reduced in vacuo to give a yellow solid (325 mg, 82%). Mp 148.0–150.0 °C. Anal. Calcd for C₁₄H₁₃BF₃NO: C, 60.26; H, 4.70; N, 5.02. Found: C, 60.29; H, 4.77; N, 4.84. 1H NMR (200 MHz), δ 8.55 (d, AA'XX', H₂ and H₆, $^3J_{HH}$ = 6.8 Hz), 7.67 (d, AA'XX', H₃ and H₅, $^3J_{HH}$ = 6.8 Hz), 7.54 (d, AA'XX', H₁₁ and H₁₃, $^3J_{HH}$ = 8.6 Hz), 7.48 (d, H₇, AB, $^3J_{HH}$ = 15.8 Hz), 6.95 (d, AB, H₈, $^3J_{HH}$ = 15.8 Hz), 6.94 (d, AA'XX', H₁₀ and H₁₄, $^3J_{HH}$ = 8.6 Hz), 3.85 (s, H₁₅); $^{13}C\{^1H\}$ NMR (50 MHz) δ 161.6 (C₁₂), 152.3 (C₄), 143.1 (C₂ and C₆), 139.1 (C₈), 129.6 (C₁₀ and C₁₄), 127.5 (C₉), 122.0 (C₃ and C₅), 120.6 (C₇), 114.7 (C₁₁ and C₁₃), 55.5 (C₁₅); $^{11}B\{^1H\}$ (64 MHz) δ 0.52 (s); $^{19}F\{^1H\}$ (188 MHz), δ -152.5 (m, broad).

trans-4-MeO-C₆H₄-C(H)=C(H)-C₅H₄N·B(C₆F₅)₃ (7b). A solution of B(C₆F₅)₃ (**1b**, 145 mg, 0.284 mmol) in toluene (5 mL) was added dropwise via pipet to a stirred solution of *trans*-4-MeO-C₆H₄-C(H)=C(H)-C₅H₄N (**3**, 60 mg, 0.284 mmol) in toluene (5 mL). The reaction mixture was stirred for 3 h at ambient temperature and reduced in vacuo to give a yellow solid (185 mg, 90%). Mp 115.0–117.0 °C (d); Anal. Calcd. for

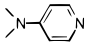
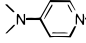
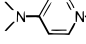
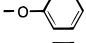
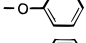
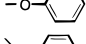
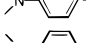
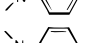
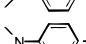
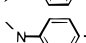
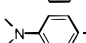

C₃₂H₁₃BF₁₅NO: C, 53.14; H, 1.81; N, 1.94. Found: C, 53.70; H, 1.76; N, 1.55. 1H NMR (200 MHz) δ 8.38 (d, AA'XX', H₂ and H₆, $^3J_{HH}$ = 6.9 Hz), 7.57 (d, AA'XX', H₃ and H₅, $^3J_{HH}$ = 6.9 Hz), 7.54 (d, AA'XX', H₁₁ and H₁₃, $^3J_{HH}$ = 8.7 Hz), 7.48 (d, H₇, AB, $^3J_{HH}$ = 16.5 Hz), 6.96 (d, AA'XX', H₁₀ and H₁₄, $^3J_{HH}$ = 8.7 Hz), 6.94 (d, AB, H₈, $^3J_{HH}$ = 16.5 Hz), 3.87 (s, H₁₅), 3.81 (minor, ca. 2%), plus toluene of crystallization; $^{13}C\{^1H\}$ NMR (50 MHz) δ 161.8, 151.6, 147.9 (dm, J_{C-F} = 244 Hz, BR₃), 146.1, 140.1 (dm, J_{C-F} = 252 Hz, BR₃), 140.0, 139.8, 137.6 (toluene), 137.2 (dm, J_{C-F} = 243 Hz, BR₃), 130.3, 129.7, 129.0 (toluene), 128.2 (toluene), 127.4, 125.3 (toluene), 125.0, 121.5, 120.3, 118.6 (br, s, BR₃), 114.7, 114.4, 55.5, 20.5 (toluene); $^{11}B\{^1H\}$ (64 MHz) δ -4.10 (s); $^{19}F\{^1H\}$ (188 MHz) δ -131.2 (s, broad, 2F), -156.7 (t, broad, 1F), -163.0 (s, broad, 2F), plus ca. -135 (trace).

trans-4-Me₂N-C₆H₄-C(H)=C(H)-C₅H₄N·BF₃ (8a). A solution of BF₃·Et₂O (**1a**, 0.8 M, 1.7 mL, 1.4 mmol) was added dropwise via pipet to a stirred solution of *trans*-4-Me₂N-C₆H₄-C(H)=C(H)-C₅H₄N (**4**, 300 mg, 1.34 mmol) in THF (5 mL). The reaction mixture was stirred overnight at ambient temperature while covered in aluminum foil. The orange precipitate was isolated by vacuum filtration, washed with hexanes (3 × 5 mL), and dried in vacuo (330 mg, 84%). Mp 198.0–199.5 °C (d). Anal. Calcd for C₁₅H₁₆BF₃N₂: C, 61.68; H, 5.52; N, 9.59. Found: C, 61.42; H, 5.57; N, 9.38. 1H NMR (200 MHz) δ 8.48 (d, AA'XX', H₂ and H₆, $^3J_{HH}$ = 6.7 Hz), 7.60 (d, AA'XX', H₃ and H₅, $^3J_{HH}$ = 6.7 Hz), 7.48 (d, AA'XX', H₁₁ and H₁₃, $^3J_{HH}$ = 8.8 Hz), 7.46 (d, H₇, AB, $^3J_{HH}$ = 16.1 Hz), 6.84 (d, AB, H₈, $^3J_{HH}$ = 16.1 Hz), 6.73 (d, AA'XX', H₁₀ and H₁₄, $^3J_{HH}$ = 8.8 Hz), 3.06 (s, H₁₅); $^{13}C\{^1H\}$ NMR (50 MHz) δ 153.0 (C₁₂), 152.7 (C₄), 142.8 (C₂ and C₆), 140.0 (C₈), 129.8 (C₁₀ and C₁₄), 122.7 (C₉), 121.4 (C₃ and C₅), 117.6 (C₇), 112.1 (C₁₁ and C₁₃), 40.2 (C₁₅); $^{11}B\{^1H\}$ (64 MHz) δ 0.74 (s); $^{19}F\{^1H\}$ (188 MHz) δ -152.7 (m, broad).

trans-4-Me₂N-C₆H₄-C(H)=C(H)-C₅H₄N·B(C₆F₅)₃ (8b). A solution of B(C₆F₅)₃ (**1b**, 137 mg, 0.268 mmol) in hexanes (5 mL) was added dropwise via pipet to a stirred solution of *trans*-4-Me₂N-C₆H₄-C(H)=C(H)-C₅H₄N (**4**, 60 mg, 0.268 mmol) in hexanes (5 mL). The reaction mixture was stirred for 2 h at ambient temperature and was reduced in vacuo to ca. 4 mL. The resultant precipitate was isolated by vacuum filtration and washed with hexanes (5 mL) to give a deep red solid (165 mg, 84%). Mp 160.5–162.0 °C. Anal. Calcd for C₃₃H₁₆-BF₁₅N₂: C, 53.83; H, 2.19; N, 3.81. Found: C, 53.53; H, 2.30; N, 3.58. 1H NMR (200 MHz) δ 8.27 (d, AA'XX', H₂ and H₆, $^3J_{HH}$ = 5.8 Hz), 7.49 (d, AA'XX', H₃ and H₅, $^3J_{HH}$ = 5.8 Hz), 7.48 (d, AA'XX', H₁₁ and H₁₃, $^3J_{HH}$ = 8.9 Hz), 7.46 (d, H₇, AB, $^3J_{HH}$ = 16.0 Hz), 6.81 (d, AB, H₈, $^3J_{HH}$ = 16.0 Hz), 6.70 (d, AA'XX', H₁₀ and H₁₄, $^3J_{HH}$ = 8.9 Hz), 3.06 (s, H₁₅), plus hexanes (1.27, 0.89 minor); $^{13}C\{^1H\}$ NMR (50 MHz) δ 154.9, 152.1, 152.0, 148.2, 147.9 (dm, J_{C-F} = 236 Hz, BR₃), 145.6, 140.6, 140.2 (dm, J_{C-F} = 234 Hz, BR₃), 137.2 (dm, J_{C-F} = 251 Hz, BR₃), 130.5, 129.9, 122.5, 120.8, 117.1, 112.0, 111.6, 40.1 (plus minor upfield resonances attributed to hexanes solvent; B–C resonances were not observed); $^{11}B\{^1H\}$ (64 MHz) δ -4.21 (s, broad); $^{19}F\{^1H\}$ (188 MHz) δ -131.3 (d, broad, 2F, J_{FF} = 19.7 Hz), -156.7 (t, broad, 1F, J_{FF} = 20.3 Hz), -163.0 (t, broad, 2F), minor component (<5%), -132.5 (d, broad, J_{FF} = 18.5 Hz), -137.0 (s, broad), -150.8 (t, broad), -155.0 (t, broad), -161.6 (s, broad), -163.6 (m, broad).

4-Me₂N-C₆H₄-C≡C-C₅H₄N·BF₃ (9a). A solution of BF₃·Et₂O (**1a**, 1.0 M, 70 mg, 0.493 mmol) was added dropwise via pipet to a stirred suspension of 4-Me₂N-C₆H₄-C≡C-C₅H₄N (**5**, 109 mg, 0.493 mmol) in Et₂O (15 mL). The reaction mixture turned bright orange immediately, and a precipitate began to form. The reaction mixture was stirred for 3 h at ambient temperature and was reduced in vacuo to ca. 5 mL. The precipitate was isolated by vacuum filtration and washed with Et₂O (2 × 5 mL) to give a bright orange solid (124 mg, 87%). Mp 135.0–136.0 °C (d). Anal. Calcd for C₁₅H₁₄BF₃N₂: C, 62.11; H, 4.86; N, 9.66. Found: C, 62.33; H, 4.87; N, 9.38. 1H NMR (200 MHz) δ 8.57 (d, AA'XX', H₂ and H₆, $^3J_{HH}$ = 6.7 Hz), 7.64 (d, AA'XX', H₃ and H₅, $^3J_{HH}$ = 6.7 Hz), 7.47 (d, AA'XX', H₁₁ and H₁₃, $^3J_{HH}$ = 9.0 Hz), 6.68 (d, AA'XX', H₁₀ and H₁₄, $^3J_{HH}$ = 9.0 Hz), 3.06 (s, H₁₅); $^{13}C\{^1H\}$ NMR (50 MHz) δ 151.6 (C₁₂), 142.6 (C₂ and C₆), 134.2 (C₁₀ and C₁₄), 126.7 (C₃

Table 1. Absorption^a and Nonlinear Optical Data^b

molecule	λ_{\max} (nm) (log ϵ)	μ_{exp} (D)	β (10^{-30} esu)	$\mu\beta$ (10^{-48} esu)	$\beta(0)$ (10^{-30} esu)	$\mu\beta(0)$ (10^{-48} esu)
	258 (3.76)	5	5.5	27.5	4.5	22.5
	276 (3.79)	5	13.6	69	11	55
	288 (4.18)	5	11.4	57	9	44.5
	326 (4.03)	6	24	144	17.2	103.2
	364 (4.07)	7.3	48	348	30.5	223
	376 (4.19)	6.45	48	310	30	194
	368 (4.23)	10	45	450	29.1	291
	438 (4.26)	11.8	129	1520	61	721.5
	458 (4.28)	10	155	1560	72.5	724
	356 (4.03)					
	422 (4.38)	10.2	60	606	31.5	321
	440 (4.45)					

^a In CHCl₃ in 10 mm cells. ^b EFISH measurements were done at 1.34 μm .

Table 2. Data Collection and Structure Solution and Refinement for 6a–c, and 9b

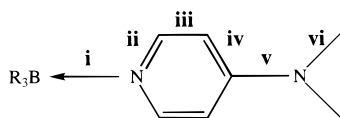
	6a	6b	6c	9b
formula	C ₇ H ₁₀ BF ₃ N ₂	C ₂₅ H ₁₀ BF ₁₅ ·2C ₇ H ₈	C ₇ H ₁₃ BN ₂	C ₃₃ H ₁₄ BF ₁₅ N ₂
MW	190.0	818.4	136.0	734.3
crystal system	orthorhombic	orthorhombic	orthorhombic	monoclinic
space group	<i>Pbca</i>	<i>Pbca</i>	<i>Pbca</i>	<i>P2₁/c</i>
<i>a</i> (Å)	10.430(3)	12.322(1)	9.6914(7)	9.833(2)
<i>b</i> (Å)	8.111(2)	20.556(2)	11.7173(9)	10.717(1)
<i>c</i> (Å)	20.295(7)	28.455(3)	22.718(2)	28.421(4)
α (deg)	90	90	90	90
β (deg)	90	90	90	91.96(1)
γ (deg)	90	90	90	90
<i>V</i> (Å ³)	1717.0(9)	7207.4(14)	1622.4(5)	2993.4(8)
<i>Z</i>	8	8	8	4
<i>d</i> _{calc} (g cm ⁻³)	1.470	1.508	1.114	1.629
crystal size (mm)	0.50{100} × 0.34{010} × 0.34{210} × 0.05{001}	0.38{110} × 0.18{001}	0.44{100} × 0.70{010} × 0.11{001}	0.76{100} × 0.38{010} × 0.22{001}
crystal color	colorless	colorless	colorless	orange-red
temp (K)	175	200	200	180
μ (cm ⁻¹)	1.34	1.42	0.66	1.61
<i>F</i> (000)	784	3312	592	1464
2 θ range (deg)	4.0–54.0	4.0–50.0	4.0–50.0	4.0–50.0
index ranges	0 ≤ <i>h</i> ≤ 13, 0 ≤ <i>k</i> ≤ 10, 0 ≤ <i>l</i> ≤ 25	0 ≤ <i>h</i> ≤ 14, 0 ≤ <i>k</i> ≤ 24, 0 ≤ <i>l</i> ≤ 33	0 ≤ <i>h</i> ≤ 12, 0 ≤ <i>k</i> ≤ 9, 0 ≤ <i>l</i> ≤ 24	0 ≤ <i>h</i> ≤ 11, 0 ≤ <i>k</i> ≤ 12, -33 ≤ <i>l</i> ≤ 33
refl measd	1884	6352	1441	5279
independent refl	1884	6352	1441	5279
refl with <i>F</i> > 6 σ (<i>F</i>)	1083	3093 (<i>F</i> > 4 σ (<i>F</i>))	882	3439
max and min transmission	0.9871, 0.9324	0.9800, 0.9576	0.9923, 0.9693	0.9664, 0.9427
extinction coeff. (γ)	0.00151(9)		0.00252(8)	0.00040(3)
no. of parameters	156	517	129	475
GOF on <i>F</i>	3.81	1.53	2.29	2.03
final <i>R</i> indexes [<i>F</i> > 6 σ (<i>F</i>)]	<i>R</i> = 0.0522 <i>wR</i> = 0.0564	<i>R</i> = 0.0465 <i>wR</i> = 0.0367	<i>R</i> = 0.0369 <i>wR</i> = 0.0362	<i>R</i> = 0.0338 <i>wR</i> = 0.0309
<i>R</i> indexes (all data) ^a	<i>R</i> = 0.0807 <i>wR</i> = 0.0574	<i>R</i> = 0.0969 <i>wR</i> = 0.0405	<i>R</i> = 0.0583 <i>wR</i> = 0.0373	<i>R</i> = 0.0540 <i>wR</i> = 0.0321
largest and mean shift/esd	0.001, 0.000	0.012, 0.001	0.024, 0.002	0.002, 0.000
largest diff. peak and hole (e Å ⁻³)	0.23, -0.19	0.36, -0.50	0.16, -0.16	0.22, -0.17

^a $R = \sum ||F_o| - |F_c|| / \sum |F_o|$, $wR = \{ \sum [w(F_o^2 - F_c^2)^2] / \sum [w(F_o^2)^2] \}^{1/2}$, GOF = $S = \{ \sum [w(F_o^2 - F_c^2)^2] / (n - p) \}^{1/2}$ for *n* reflections and *p* parameters in the refinement.

and C₅), 111.6 (C₁₁ and C₁₃), 40.0 (C₁₅); ¹¹B{¹H} (64 MHz) δ 0.40 (s); ¹⁹F{¹H} (188 MHz), δ -162.2 (m, broad).

4-Me₂N-C₆H₄-C≡C-C₅H₄N·B(C₆F₅)₃ (9b). A solution of B(C₆F₅)₃ (**1b**, 161 mg, 0.315 mmol) in toluene (5 mL) was added dropwise via pipet to a stirred suspension of 4-Me₂N-C₆H₄-

C≡C-C₅H₄N (**5**, 70 mg, 0.315 mmol) in toluene (5 mL). The reaction mixture turned bright orange immediately and was stirred overnight at ambient temperature. The reaction mixture was reduced in vacuo to ca. 5 mL, and hexanes (10 mL) was added to induce precipitation of the product. This

Table 3. Selected Bond Lengths (Å) for Compounds 2,²² 6a–c, and 9b^a


compound	i	ii	iii	iv	v	vi
2		1.335(3) 1.337(3)	1.381(3) 1.375(3)	1.403(2) 1.404(3)	1.367(2)	1.452(3) 1.452(3)
6c	1.594(3)	1.345(3) 1.351(3)	1.373(3) 1.365(3)	1.404(3) 1.413(3)	1.346(3)	1.451(3) 1.450(3)
6a	1.589(5)	1.354(5) 1.356(5)	1.364(5) 1.360(5)	1.422(5) 1.408(5)	1.341(4)	1.460(5) 1.463(5)
6b	1.602(6)	1.352(5) 1.349(5)	1.354(6) 1.340(6)	1.409(6) 1.414(6)	1.348(6)	1.467(6) 1.453(6)
9b	1.620(3)	1.348(3) 1.341(3)	1.362(3) 1.371(3)	1.387(3) 1.392(3)		

^a **2** = DMAP; **6a** = DMAP·BF₃; **6b** = DMAP·B(C₆F₅)₃; **6c** = DMAP·BH₃; **9b** = Me₂N–C₆H₄–C≡C–C₅H₄N·B(C₆F₅)₃.

was unsuccessful, and the reaction mixture was reduced in vacuo and analyzed by NMR. Initial NMR analysis indicated that the reaction was incomplete. The residue was suspended in hexanes (5 mL) and an additional solid portion of B(C₆F₅)₃ (20 mg) was added. The precipitate thus formed, was isolated by vacuum filtration and washed with hexanes (2 × 5 mL) to give a bright orange solid (149 mg, 65%). Mp 156.0–158.0 °C (d). Anal. Calcd for C₃₃H₁₄BF₁₅N₂: C, 53.98; H, 1.92; N, 3.82. Found: C, 53.88; H, 1.96; N, 3.63. ¹H NMR (200 MHz) δ 8.37 (d, AA'XX', H₂ and H₆, ³J_{HH} = 6.9 Hz), 7.52 (d, AA'XX', H₃ and H₅, ³J_{HH} = 6.9 Hz), 7.46 (d, AA'XX', H₁₁ and H₁₃, ³J_{HH} = 9.0 Hz), 6.67 (d, AA'XX', H₁₀ and H₁₄, ³J_{HH} = 9.0 Hz), 3.06 (s, H₁₅); ¹¹B{¹H} (64 MHz) δ –2.77 (s); ¹⁹F{¹H} (188 MHz) δ –141.9 (d, 2F, J_{FF} = 20.2 Hz), –166.9 (t, 1F, J_{FF} = 18.9 Hz), –173.4 (t, broad, 2F).

X-ray Crystallography

Crystal data and other information on structure determination are given in Table 2 for compounds **6a–c**, and **9b**. Measurements were made on a Siemens P4 four-circle diffractometer and graphite-monochromated Mo Kα radiation was used (λ = 0.710 73 Å). Crystals were obtained by slow evaporation of CDCl₃ solutions for **6a** and **6c** and by slow evaporation of mixed toluene/hexanes solutions for **6b** and **9b**. The crystals were mounted on glass fibers with epoxy cement, cell parameters were refined from the observed setting angles of selected reflections, and intensities were measured with ω scans.

The structures were solved by direct methods and refined by full-matrix least-squares techniques. The refinement was on *F* of reflections with *F*_o > 6σ(*F*_o) (*F*_o > 4σ(*F*_o)) for **6b**) to minimize Σw(|*F*_o – |*F*_c||², with weighting *w*^{–1} = σ²(*F*_o); the refined isotropic extinction parameter *χ* is defined such that *F*_c is multiplied by (1 + 0.002*χF*_o²/sin 2θ)^{–1/4}. In each case, anisotropic displacement parameters were refined for all non-hydrogen atoms, and isotropic hydrogen atoms were constrained to ride on their parent carbon atoms with fixed bond lengths and idealized bond angles.

In the structure of **6a**, 2-fold disorder was present in the BF₃ group. Programs were standard Siemens control and integration software, version 4 of SHELXTL, and local programs. For the structure of **6b**, hydrogen isotropic thermal parameters were refined as three common variables. In the case of **6c**, the compound was assumed to be isostructural with **6a** and the B–H proton coordinates were refined. In addition, because of diffractometer phi-drive problems, normal measurement of standard reflections was not possible. Monitoring of a few repeat data, however, indicated only very minor fluctuations of intensity.

Refined atomic coordinates and selected bond lengths are given in Tables 2 and 3, respectively. Atomic coordinates and equivalent isotropic displacement parameters are given in Tables 4–7. Complete bond lengths and angles, anisotropic

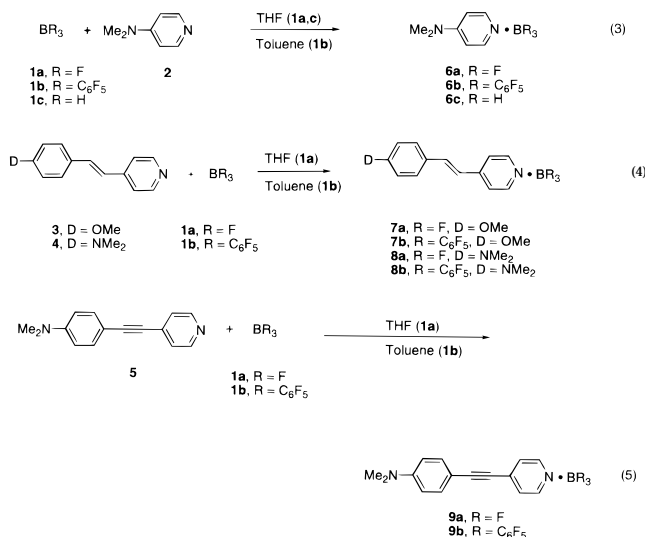
Table 4. Atomic Coordinates (×10⁴) and Equivalent Isotropic Displacement Parameters (Å² × 10³) for 6a

	<i>x</i>	<i>y</i>	<i>z</i>	<i>U</i> (eq)
N(1)	3835(3)	2119(3)	2875(1)	32(1)
C(1)	2896(4)	1230(5)	2582(2)	34(1)
C(2)	2811(4)	1020(5)	1916(2)	34(1)
C(3)	3753(4)	1731(5)	1497(2)	33(1)
C(4)	4729(4)	2637(5)	1811(2)	35(1)
C(5)	4734(4)	2803(5)	2477(2)	34(1)
B(1)	3912(5)	2335(6)	3652(2)	36(1)
F(1A)**	3734(20)	908(15)	3941(6)	90(6)
F(1B)**	4653(7)	1115(10)	3887(3)	83(3)
F(2A)**	5083(10)	2974(26)	3808(5)	95(7)
F(2B)**	4377(9)	3840(8)	3776(3)	91(3)
F(3A)**	3045(14)	3394(20)	3819(5)	84(6)
F(3B)**	2721(5)	2201(12)	3911(3)	89(3)
N(2)	3709(3)	1569(4)	840(1)	36(1)
C(6)	2713(4)	588(6)	521(2)	50(2)
C(7)	4765(4)	2178(6)	433(2)	50(2)

displacement coefficients, H-atom coordinates and isotropic displacement coefficients, and structure factor tables for the structures are available as Supporting Information.

Results and Discussion

In general, the Lewis acidic boranes BF₃ (**1a**) and B(C₆F₅)₃ (**1b**) react readily with the pyridine moiety in 4-Me₂N–C₅H₄N (DMAP, **2**; eq 3), the stilbazoles (E)-4-



D–C₆H₄–C(H)=C(H)–C₅H₄N (D = MeO (**3**), Me₂N (**4**), eq 4) and the related alkyne derivative, 4-Me₂N–C₆H₄–

Table 5. Atomic Coordinates ($\times 10^4$) and Equivalent Isotropic Displacement Parameters ($\text{\AA}^2 \times 10^3$) for 6b

	<i>x</i>	<i>y</i>	<i>z</i>	<i>U</i> (eq)
F(9)	-493(2)	4507(1)	259.3(8)	42.8(9)
F(10)	-1459(2)	4620(1)	1088.7(8)	50.7(9)
F(11)	-2396(2)	3566(1)	1500.9(8)	52.0(9)
F(12)	-2368(2)	2401(1)	1052.1(8)	52(1)
F(13)	-1415(2)	2274(1)	226.2(8)	45.5(9)
F(15)	-672(2)	2814(1)	-1296.3(8)	46.9(9)
F(16)	-203(2)	1633(1)	-1580.0(8)	60(1)
F(17)	758(2)	760(1)	-988.6(9)	63(1)
F(18)	1295(2)	1136(1)	-103.5(9)	56(1)
F(19)	854(2)	2338(1)	191.5(8)	45.7(9)
F(21)	1026(2)	3711(1)	-1136.5(7)	43.5(9)
F(22)	3021(2)	4183(1)	-1185.4(9)	60(1)
F(23)	4166(2)	4437(1)	-385.5(9)	64(1)
F(24)	3249(2)	4191(1)	462.4(8)	57(1)
F(25)	1273(2)	3716(1)	526.5(8)	45.7(9)
N(1)	-1035(3)	3766(2)	-629(1)	30(1)
N(2)	-3334(3)	4758(2)	-1430(1)	47(2)
C(1)	-871(3)	4381(2)	-776(1)	34(2)
C(2)	-1607(3)	4725(2)	-1028(1)	37(2)
C(3)	-2606(4)	4444(2)	-1158(1)	38(2)
C(4)	-2783(3)	3810(2)	-982(1)	43(2)
C(5)	-2017(3)	3507(2)	-729(1)	38(2)
C(6)	-3118(4)	5408(2)	-1607(2)	59(2)
C(7)	-4357(4)	4442(3)	-1561(2)	75(2)
C(8)	-825(3)	3377(2)	209(1)	28(1)
C(9)	-928(3)	3960(2)	449(1)	32(2)
C(10)	-1423(3)	4034(2)	874(1)	34(2)
C(11)	-1897(3)	3506(2)	1085(1)	34(2)
C(12)	-1875(3)	2923(2)	859(2)	34(2)
C(13)	-1362(3)	2870(2)	431(1)	32(2)
C(14)	4(3)	2636(2)	-521(1)	30(2)
C(15)	-213(3)	2418(2)	-973(2)	35(2)
C(16)	34(3)	1802(2)	-1133(2)	39(2)
C(17)	512(3)	1365(2)	-841(2)	42(2)
C(18)	778(3)	1554(2)	-392(2)	38(2)
C(19)	537(3)	2178(2)	-253(1)	34(2)
C(20)	1002(3)	3709(2)	-306(1)	29(1)
C(21)	1539(3)	3840(2)	-723(2)	34(2)
C(22)	2570(4)	4084(2)	-762(2)	39(2)
C(23)	3144(3)	4211(2)	-360(2)	42(2)
C(24)	2680(3)	4088(2)	62(2)	35(2)
C(25)	1645(3)	3841(2)	86(2)	34(2)
B(1)	-199(4)	3367(2)	-307(2)	31(2)
Solvent (Toluene)				
C(26)	4598(7)	-370(5)	2337(3)	124(5)
C(27)	4689(8)	240(5)	2093(2)	119(4)
C(28)	3961(11)	692(5)	2237(4)	178(7)
C(29)	3094(13)	689(8)	2557(4)	219(10)
C(30)	3161(7)	65(6)	2756(3)	146(6)
C(31)	3790(6)	-470(4)	2678(2)	89(3)
C(32)	5245(7)	-858(5)	2227(3)	169(6)
C(33)	3609(9)	7453(4)	2322(3)	128(5)
C(34)	4617(7)	7246(3)	2190(3)	107(4)
C(35)	4962(6)	7341(3)	1732(3)	122(4)
C(36)	4256(8)	7663(4)	1417(3)	103(4)
C(37)	3242(7)	7865(3)	1580(4)	109(4)
C(38)	2878(9)	7760(4)	2047(4)	150(5)
C(39)	3296(7)	7319(3)	2803(3)	198(6)

$\text{C}\equiv\text{C}-\text{C}_5\text{H}_4\text{N}$ (**5**; eq 5) in the appropriate solvent. The synthesis of $\text{DMAP}\cdot\text{BH}_3$ (**6c**) was investigated to elucidate the regioselectivity of the borane addition.

The isolation of products derived from reactions involving BF_3 (**1a**) were facilitated by precipitation of the desired adducts (**6a**, **7a**, **8a**, **9a**) from THF or Et_2O . The isolation of the adducts with $\text{B}(\text{C}_6\text{F}_5)_3$ (**1b**) were not always as straightforward. The isolation of $\text{DMAP}\cdot\text{B}(\text{C}_6\text{F}_5)_3$ (**6b**) was enhanced by precipitation with hexanes. The compound $4\text{-Me}_2\text{N}-\text{C}_6\text{H}_4-\text{C}(\text{H})=\text{C}(\text{H})-\text{C}_5\text{H}_4\text{N}\cdot\text{B}(\text{C}_6\text{F}_5)_3$ (**8b**) precipitated immediately upon addition of compound **1b** to the hexanes solution containing the stilbazole; however, reactions with the

Table 6. Atomic Coordinates ($\times 10^4$) and Equivalent Isotropic Displacement Parameters ($\text{\AA}^2 \times 10^3$) for 6c

	<i>x</i>	<i>y</i>	<i>z</i>	<i>U</i> (eq)
N(1)	3858(2)	2289(2)	2914.9(9)	327(6)
C(1)	2914(2)	1423(3)	2603(1)	350(8)
C(2)	2851(2)	1244(3)	1926(1)	331(8)
C(3)	3814(2)	1968(3)	1517(1)	309(8)
C(4)	4789(2)	2874(3)	1850(1)	351(8)
C(5)	4773(2)	2999(3)	2526(1)	360(8)
N(2)	3795(2)	1828(2)	850.9(9)	371(7)
C(6)	2817(3)	803(4)	521(1)	516(11)
C(7)	4871(3)	2450(4)	461(1)	518(11)
B(1)	3917(4)	2486(5)	3702(1)	460(11)

Table 7. Atomic Coordinates ($\times 10^4$) and Equivalent Isotropic Displacement Parameters ($\text{\AA}^2 \times 10^3$) for 9b

	<i>x</i>	<i>y</i>	<i>z</i>	<i>U</i> (eq)
F(17)	2926(1)	2044(1)	1741.1 (4)	453(5)
F(18)	1273(2)	162(1)	1930.0(5)	618(6)
F(19)	1228(2)	-1921(1)	1390.2(6)	703(7)
F(20)	2861(2)	-2070(1)	642.7(5)	699(7)
F(21)	4426(2)	-161(1)	420.3(5)	524(5)
F(23)	5779(2)	1610(2)	1856.3(5)	559(6)
F(24)	6459(2)	3183(2)	2548.0(5)	760(7)
F(25)	6270(2)	5698(2)	2405.4(6)	838(8)
F(26)	5424(2)	6569(2)	1544.2(6)	774(7)
F(27)	4745(2)	5032(1)	858.2(5)	507(5)
F(29)	6384(2)	-232(2)	1141.5(5)	644(6)
F(30)	8895(2)	-716(2)	908.5(7)	896(8)
F(31)	10316(2)	922(2)	382.0(7)	860(8)
F(32)	9082(2)	3064(2)	76.1(6)	707(7)
F(33)	6595(1)	3617(1)	338.2(5)	487(5)
N(1)	3915(2)	2740(2)	490.2(6)	257(6)
N(2)	-1498(2)	6689(2)	-2604.3(7)	475(8)
C(1)	4160(2)	2503(2)	37.6(7)	291(8)
C(2)	3346(2)	2951(2)	-325.5(8)	328(8)
C(3)	2226(2)	3683(2)	-229.9(8)	313(8)
C(4)	1958(2)	3894(2)	241.1(8)	332(8)
C(5)	2793(2)	3403(2)	585.7(7)	310(8)
C(6)	1417(2)	4223(2)	-606.0(8)	374(9)
C(7)	824(2)	4687(2)	-934.6(9)	389(9)
C(8)	168(2)	5254(2)	-1337.3(8)	357(8)
C(9)	790(3)	6220(3)	-1572.9(9)	509(10)
C(10)	242(3)	6719(3)	-1981.7(9)	484(10)
C(11)	-970(2)	6242(2)	-2183.2(8)	367(9)
C(12)	-1627(3)	5309(2)	-1933.7(7)	411(9)
C(13)	-1071(3)	4833(2)	-1521.7(8)	389(9)
C(14)	-859(3)	7718(3)	-2837(1)	632(13)
C(15)	-2756(4)	6199(3)	-2795(1)	783(15)
C(16)	3832 (2)	1016(2)	1084.7(7)	299(8)
C(17)	2966(2)	1035(2)	1458.8(8)	331(8)
C(18)	2097(3)	79(2)	1563.7(8)	403(9)
C(19)	2064(3)	-974(2)	1290.8(9)	459(10)
C(20)	2877(3)	-1038(2)	913.6(9)	443(9)
C(21)	3697(3)	-52(2)	815.4(8)	373(9)
C(22)	5153(2)	3218(2)	1325.4(8)	325(8)
C(23)	5644(3)	2843(3)	1768.5(8)	406(9)
C(24)	6011(3)	3639(3)	2129.4(9)	518(11)
C(25)	5926(3)	4905(3)	2056(1)	566(12)
C(26)	5493(3)	5337(3)	1627(1)	516(11)
C(27)	5137(3)	4500(2)	1273.4(8)	397(9)
C(28)	6330(2)	1720(2)	746.0(8)	338(8)
C(29)	7012(3)	641(3)	879.7(8)	465(10)
C(30)	8323(3)	366(3)	763(1)	591(12)
C(31)	9030(3)	1189(3)	496(1)	570(12)
C(32)	8423(3)	2265(3)	349(1)	486(10)
C(33)	7120(2)	2514(2)	483.9(8)	382(9)
B(1)	4818(3)	2155(3)	923.7(9)	292(9)

methoxy stilbazole derivative **3** and **1b** were incomplete in hexanes. When reactions involving the stilbazoles were carried out using toluene as solvent, the products were very soluble and complete removal of solvent was difficult. Extended periods of drying under vacuum were necessary to obtain the product in the solid state. These reactions were assumed to have reached comple-

tion due to the rapid color change observed and the absence of precursors in spectroscopic characterization. For example, addition of **1b** to **3** and **4** resulted in either a very intense yellow (**7b**) or red (**8b**) color, respectively. Similarly, the reaction involving compound **1b** with the alkyne derivative (**5**) proceeded readily in toluene accompanied by the formation of a deep red color; however, reactions in hexanes appear to be optimal in regards to the isolation of the product (**9b**).

A variety of techniques was used to characterize the compounds prepared in this study. Melting point determinations, elemental analyses and yields are presented in the Experimental Section with multinuclear NMR (^1H , ^{11}B , ^{13}C , and ^{19}F) results. In addition, UV/vis spectroscopic analysis and selected NLO measurements are presented (Table 1). The DMAP derivatives (**6a–c**) and compound **9b** have been structurally characterized using X-ray crystallography, and crystal data and selected bond lengths are summarized in Tables 2 and 3. Tables of atomic coordinates and equivalent isotropic displacement parameters for the compounds are given in Tables 4–7.

The majority of compounds studied melt with apparent decomposition. The temperature at which decomposition became apparent in the sample is noted for compounds denoted by (d). The values determined for the adducts involving $\text{B}(\text{C}_6\text{F}_5)_3$ are quite low in several cases. However, an efficient NLO compound such as **8a** is stable up to 200 °C. Elemental analyses are consistent with the proposed structures of the products with minor differences attributed to incomplete burning of samples or slight deviations due to strongly bound solvent. The $\text{B}(\text{C}_6\text{F}_5)_3$ derivatives appear to be less stable than the BF_3 analogues in most cases. In addition, analysis of **5** was hampered by a trace amount of the homocoupled pyridine–acetylene product which was separated upon coordination of the Lewis acid groups.

The stilbazole derivatives were not prone to photolytic degradation or isomerization according to NMR studies. The compounds did however exhibit signs of irreversible degradation in solutions exposed to air when examined by UV/vis spectroscopy.

The NMR results were also consistent with the presence of solvent in the products isolated in reactions with $\text{B}(\text{C}_6\text{F}_5)_3$. Generally, there were traces of solvent present in the ^1H and ^{13}C NMR spectra of the compounds initially isolated; however, after extended periods of drying under vacuum, satisfactory spectra were obtained. The compounds **5**, **9a**, and **9b** were only sparingly soluble in CDCl_3 , and this resulted in the incomplete characterization of these compounds by $^{13}\text{C}\{-^1\text{H}\}$ NMR spectroscopy.

The DMAP derivatives (**6a–c**) display NMR resonances different from the parent molecule (**2**) due to the redistribution of charge and subsequent changes in shielding of nuclei due to the binding of the various boranes (**1a–c**). ^1H NMR spectra of the compounds display typical chemical shifts for H_2 and H_6 , which are the furthest downfield at ca. δ 8–9 ppm as has been noted for the stilbazolium salts studied.³ The ^1H and $^{13}\text{C}\{-^1\text{H}\}$ NMR spectra of the stilbazole derivatives were assigned from a comparison with previous work (^1H)^{13b} and calculated values (^{13}C).¹⁸ The coupling between the

olefinic hydrogens (**7a**, $^3J_{\text{H-H}} = 15.8$ Hz) is typical for a trans configuration about the double bond.³ The $\text{B}(\text{C}_6\text{F}_5)_3$ ligands exhibit coupling to both the ^{19}F and ^{11}B nuclei giving rise to doublets of multiplets in the $^{13}\text{C}\{-^1\text{H}\}$ NMR spectra. Slight dissociation of the $\text{B}(\text{C}_6\text{F}_5)_3$ ligand or possibly, isomerization complicated the ^{13}C NMR spectra of **7b** and **8b**. This resulted in the incomplete assignment of the resonances attributed to these products.

The UV/vis studies can be used to determine the changes in the electronic structure of the new materials. The changes in the value of the lowest energy charge-transfer transition (λ_{max}) are summarized in Table 1. The peaks corresponding to λ_{max} are attributed to the intramolecular charge-transfer transition to the lowest energy excited state. This transition emanates from the donor end of the molecule and subsides on the acceptor end.^{7c} Thus, by coordinating the electron-withdrawing groups we observe an increase in the value of λ_{max} (red shift) consistent with an increase in the acceptor strength. The molar absorptivity constant, ϵ , in these measurements should be considered only qualitatively, as the small amounts (5–10(\pm 1) mg) of sample employed give rise to limited accuracy (\pm 10–20%).

The molecular hyperpolarizabilities (β) of selected derivatives (Table 1) were determined by the electric field induced second harmonic generation (EFISH) method. The measurements were made in CHCl_3 solutions at a fundamental wavelength of 1.34 μm . It is apparent from Table 1 that the coordination of the Lewis acidic boranes results in enhanced values of $\mu\beta$ by a factor of >2 in all cases. The values for the derivatives containing BF_3 are larger with the exception of the (dimethylamino)stilbazole derivatives in which the values are similar. Although the CT excited states are at lower energy for those compounds involving the $\text{B}(\text{C}_6\text{F}_5)_3$ acceptor group, the experimentally determined values of the dipole moments indicate that the ground-state charge transfer is slightly less efficient in these compounds. This may be a result of partial dissociation of the bulky acceptor group for the samples in solution. The values ($\mu\beta$) for compounds **7a,b** (348×10^{-48} esu (**7a**); 310×10^{-48} esu (**7b**)) are lower than those for compounds **8a,b** (1520×10^{-48} esu (**8a**); 1560×10^{-48} esu (**8b**)) as expected from the presence of the weaker donor substituent MeO .^{5d} The values of $\mu\beta(0)$ also follow a similar trend.¹⁹ The values determined indicate a stronger response for the stilbazole derivatives as would be expected from previous studies involving variation in the unsaturated backbone for a series of similar compounds.²⁰ Comparison with the well-known dyes DANS (dimethylamino)nitrostilbene; $\lambda_{\text{max}} = 427$ nm (CHCl_3); $\mu\beta(0) = 1000 \times 10^{-48}$ esu) and DR1 (disperse red 1; $\lambda_{\text{max}} = 455$ nm; $\mu\beta(0) = 500 \times 10^{-48}$ esu) indicate

(18) ^{13}C NMR chemical shifts were calculated using a module developed for Chem Window 3.0.0 by Dr. Ernő Pretsch, Department of Organic Chemistry, ETH, Zurich, Switzerland, 1990–1993 Softshell International Ltd.

(19) Both $\mu\beta$ and $\mu\beta(0)$ are given since the two-level model may not be accurate for these compounds due to the possible presence of low-lying excited states that may contribute to β .

(20) Recently, a study involving ammonium/borate zwitterions has been reported in which phenyl, olefinic, and alkynyl backbones were examined for second-order NLO efficiency: Lambert, C.; Stadler, S.; Bourhill, G.; Bräuchle, C. *Angew. Chem., Int. Ed. Engl.* **1996**, *35*, 644.

similar (or even 1.5 times higher for dimethylamino derivatives) efficiency in terms of NLO effects as well as transparency for compounds **8a** ($\lambda_{\max} = 438$ nm (CHCl₃); $\mu\beta(0) = 721.5 \times 10^{-48}$ esu) and **8b** ($\lambda_{\max} = 458$ nm (CHCl₃); $\mu\beta(0) = 724 \times 10^{-48}$ esu).

The enhancement in NLO efficiency of the current materials is comparable to that observed upon coordination of W(CO)₅ to (dimethylamino)stilbazole. In the current study, the enhancement was not as significant (increasing by a factor of 3); however, the authors did note that a significant portion of the response for the metal compound was due to a large increase in dipole moment. This does not appear to be the case with the Lewis acid derivatives studied here.

Kurtz and Perry powder tests^{21a} for a rough evaluation of SHG efficiency in the crystalline state were performed at 1.06 and 1.34 μm . Only compounds **3** and **7b** displayed a detectable SHG signal (close to that of 3-methyl-4-nitropyridine 1-oxide (POM = 13 \times urea) and of KDP (= 0.33 \times urea), respectively).^{21b} All other compounds are SHG inactive. The crystal data and details of the structural determinations are summarized in Table 2 for compounds **6a–c** and **9b** (Figures 2–5, respectively). All of them belong to centrosymmetric space groups. Selected bond distances for the compounds are given in Table 3. Single crystals of the stilbazole derivatives suitable for X-ray crystallography could not be obtained in several attempts. The electronic perturbations apparent in the UV/vis studies are also apparent in the solid-state structures of the compounds to a small degree. In particular, comparisons between the DMAP derivatives (**6a–c**), show distortions upon coordination with stronger Lewis acids, which are consistent with a very slight deviation toward the quinoidal resonance structure associated with the charge-transfer excited state and therefore with the improvement of the NLO properties upon complexation.

The distortions described are prevalent to the largest extent in the bond distances in the aryl moiety of the structures. The structure of DMAP has been reported²² and has been included in Table 3 for the purpose of comparison. The pyridyl moiety is virtually planar in all cases, as expected for an aromatic compound, and the bond distances around the ring vary slightly due to the different atomic radius of the heteroatom. As a result, the bond distances denoted by **ii** in Table 3 are smaller than other distances within the ring. The onset of a quinoidal resonance form should be most prevalent as a shortening in the bond distances between atoms C(1), C(2), and C(4), C(5) (denoted as **iii**, Table 3), since the double bonds of the resonance form would be concentrated in this region of the ring. Comparing the DMAP adducts in order of acceptor strength (B(C₆F₅)₃ (**6b**) > BF₃ (**6a**) > BH₃ (**6c**)) indicates that this effect is indeed present with the largest difference in these bond distances occurring between the structures of compound **6b** (1.354(6) and 1.340(6) Å) and the parent molecule DMAP (**2**) (1.381(3) and 1.375(3) Å). A similar effect may be apparent in the bond distances denoted by **ii**

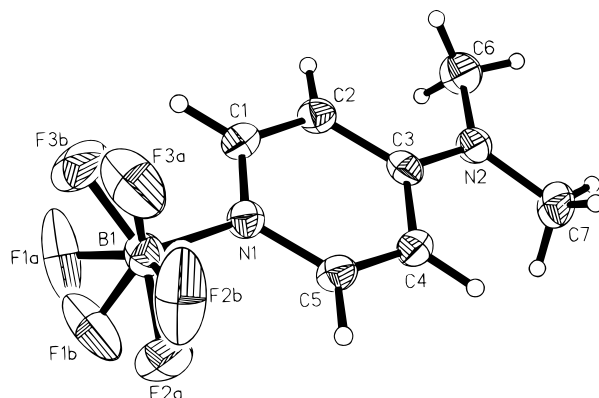


Figure 2. Molecular structure of 4-Me₂N-C₅H₄N·BF₃ (**6a**), with 50% probability ellipsoids.

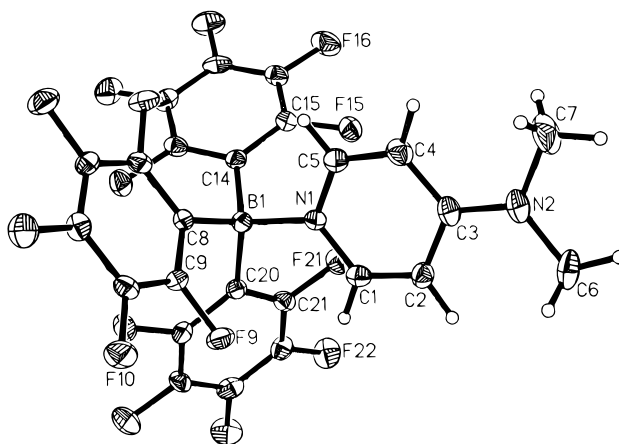


Figure 3. Molecular structure of 4-Me₂N-C₅H₄N·B(C₆F₅)₃ (**6b**), with 50% probability ellipsoids.

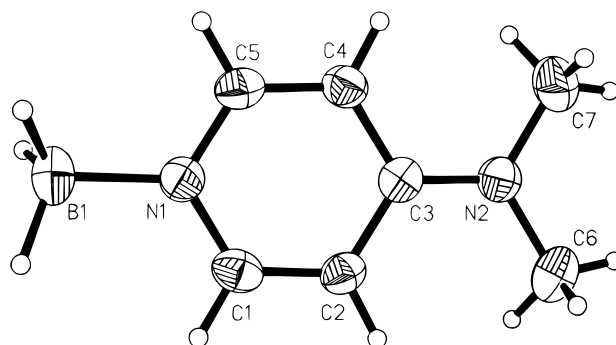


Figure 4. Molecular structure of 4-Me₂N-C₅H₄N·BH₃ (**6c**), with 50% probability ellipsoids.

(Table 3); however, the effect is not as drastic, and values are virtually equivalent within a 3 σ range.

In the structure of **9b** (Figure 5), the increase in the acceptor strength upon coordination of B(C₆F₅)₃ is not manifested in changes in the pyridyl moiety due to the presence of the extended π -system between the ends of the molecule. The C(6)–C(7) bond distance (1.192(3) Å) is consistent with a triple bond. The relatively long B–N bond (**i**) for this compound demonstrates the weaker interaction of the sterically hindered B(C₆F₅)₃ group, and this may account for dissociative effects in solution which lead to weaker dipole moments and lower efficiency in charge-transfer processes demonstrated with this series of compounds relative to the BF₃ analogues. Comparison of the B–N bond distances (**i**) in the series of compounds derived from DMAP clearly

(21) (a) Kurtz, S. K.; Perry, T. T. *J. Appl. Phys.* **1968**, *39*, 3798. (b) Zyss, J.; Chemla, D. S.; Nicoud, J. F. *J. Chem. Phys.* **1981**, *74*, 4800.

(22) (a) Ohms, U.; Guth, H. *Z. Kristallogr.* **1983**, *162*, 174. (b) Ohms, U.; Guth, H. *Z. Kristallogr.* **1984**, *166*, 213.

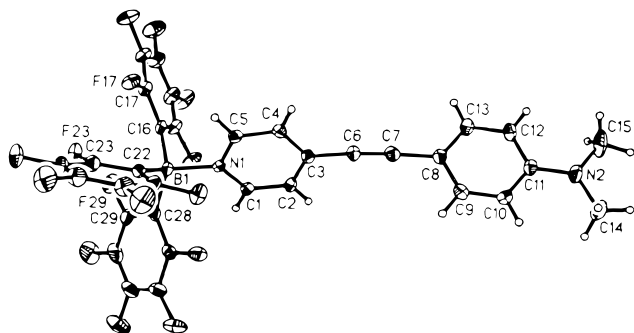


Figure 5. Molecular structure of 4-Me₂N-C₆H₄-C≡C-C₅H₄N·B(C₆F₅)₃ (**9b**), with 50% probability ellipsoids.

demonstrate this effect in the solid state with values ranging from 1.589(5) Å for the BF₃ derivative (**6a**) to 1.602(6) Å for the B(C₆F₅)₃ derivative (**6b**).

Conclusions

The synthesis and characterization of a series of new, highly polar chromophores have been described. The characterization of the new materials prepared in this study indicate that there is good electronic communication in the chromophores with coordinated Lewis-acidic boranes, BF₃ and B(C₆F₅)₃. UV/vis studies indicate a red shift upon coordination which is consistent with a reduction in the energy necessary to reach the charge-transfer excited state. The structural studies are also consistent with the UV/vis studies. Coordination of the

various boranes to the chromophore DMAP resulted in structural distortions that corroborate the solution studies. The EFISH experiments indicate considerable increases in the values of the molecular dipole moments and the second-order NLO coefficients upon complexation with the strong Lewis acids, the largest values being realized for the (dimethylamino)stilbazole derivatives. Values for $\mu\beta$ were increased by a factor of greater than 2 in most cases and lead to a significant increase of $\beta(0)$ values (up to 50%) as compared to the DR1 standard molecules. Although many of the compounds studied do not exhibit suitable thermal stability, the NLO response of amorphous polymers functionalized with efficient and stable molecules such as **8a** is expected to be comparable or higher than that of the best DR1-functionalized EO polymers.

Acknowledgment. We thank NSERC of Canada for research support (T.B.M.), SERC of UK for postgraduate support (A.T.), Arnaud Bozec for assistance with EFISH measurements, and Prof. M. Baird for generously providing initial samples of B(C₆F₅)₃ used in this study.

Supporting Information Available: Complete bond lengths and angles, anisotropic displacement coefficients, H-atom coordinates and isotropic displacement coefficients, and structure factor tables for the structures (55 pages). Ordering information is given on any current masthead page.
CM9707519